Proceedings of FEDSM'98:
1998 ASME Fluids Engineering Division Summer Meeting
June 21-25, 1998, Washington, DC

FEDSM98-4806

AIR ENTRAINMENT BY TWO-DIMENSIONAL PLUNGING JETS : THE IMPINGEMENT REGION AND THE VERY-NEAR FLOW FIELD

H. CHANSON
Department of Civil Engineering
The University of Queensland
Brisbane QLD 4072, Australia

T. BRATTBERG
Department of Civil Engineering
The University of Queensland
Brisbane QLD 4072, Australia

ABSTRACT

In the developing flow region of a plunging jet, the very-near field (i.e. $(x-x_1)/d_1 < 5$) is strongly affected by the entrapment process at the impingement. New quantitative results show that, although the distributions of void fraction and mean velocity have smooth shapes, the flow is highly fluctuating and unstable. At a given location in the mixing layer, the probability distribution function of the mean velocity exhibits two distinctive peaks : the jet impact velocity and the induction trumpet velocity. The water velocity fluctuates between the two characteristic values.
Keywords : plunging jet, air entrainment, turbulent shear flow, very-near flow field, interaction bubble-turbulence.

INTRODUCTION

At the intersection of a free-falling jet with a pool of liquid, air can be entrained and transported downwards. In industrial applications, the process is commonly used with plunging jet columns, drop structures in waterways, cooling system of power plants.

Review on plunging jet flows

Plunging jet entrainment takes place when the jet impact velocity exceeds a critical velocity. The onset velocity is a function of the jet turbulence. For small jet velocities larger than the onset velocity, air is entrained in the form of individual air bubbles. At larger jet velocities, large air packets are entrained and broken up subsequently in the shear flow.

The near-flow field is characterised by the developing shear layer and air diffusion layer (fig. 1). Recent experimental results with vertical supported jets have shown that these layers do not coincide (CHANSON 1995, CUMMINGS 1996, CHANSON and BRATTBERG 1997). Below the impingement point, the air entrainment is primarily an advection-diffusion process and most air is entrained in the region of high-velocity ($V > V_1/2$). Although the velocity distribution has the same shape as for monophase flows, the quantitative parameters are affected by the presence of entrained air bubbles.

The presence of bubbles modifies the momentum transfer within the shear layer. The turbulent shear contributes to the bubble breakage, leading to a broad spectrum of bubble sizes in the shear flow. Overall the developing flow region of plunging jets is subjected to strong interactions between the entrained air bubbles and the momentum transfer mechanism.

Purpose of the present work

Recent reviews (BIN 1993, CHANSON 1997) emphasised the absence of information on the near and very-near flow field. CHANSON (1997) suggested that, in the developing flow region of a plunging jet, the entrained air bubbles are advected downwards by a "turbulent diffusion" process. It was emphasised however that "such an assumption does not reflect the real nature of the turbulent shear layer nor the existence of vortical structures" and the theoretical results "are not valid very-close to the entrainment point" (CUMMINGS and CHANSON 1997).

In the paper, the authors will describe a new study of the very-near flow field defined as $(x-x_1)/d_1 < 5$. It is the purpose of this work to describe quantitatively the mechanisms of air entrapment and the interactions between gas and liquid entrainment.

EXPERIMENTAL INVESTIGATIONS

Experimental apparatus

Experimental investigations were conducted in the two-dimensional supported plunging jet experiment previously used by CHANSON (1995), CUMMINGS (1996) and CHANSON and BRATTBERG (1997). The apparatus consists of a glass tank (1.8-m deep, 0.30-m wide) and a vertical nozzle supplying a 2-D supported jet. The support characteristics are : 0.269-m width and 0.35-m support length. The water supply comes from a constant head tank and the jet thickness at nozzle is 0.012-m. Domestic water was used in all experiments (table 1).

Instrumentation

Velocities were measured using a Pitot tube (in clear water) and a conical hot-film probe system in air-water flow. The latter used a special miniature probe Dantec 55R42 (0.3-mm size) scanned at 40 kHz.

A double-tip conductivity probe was used to record air content, bubble frequency and chord lengths. The probe consists of two identical tips (internal ∅ 25 μm, external ∅ 200 μm) spaced 8-mm apart, scanned at 10 to 40 kHz per channel.

The displacement of the probes in the flow direction and direction normal to the jet support was controlled by two fine adjustment travelling mechanisms and measured with two Lucas Schaevitz Magnarules Plus™ MRU-012 and MRU-036. Overall the error in the probe position was less than 0.1 mm in each direction.

Additional information was obtained by visual observations using high-speed photographs.

Further details of the experimental apparatus and instrumentation were reported in CHANSON and BRATTBERG (1997).

Data processing. In air-water flow, velocity measurements with hot-film probes require the distinction between air and water phases. A new processing technique was developed to record only the water phase velocity. The air bubble signals were discriminated using a method based on one signal threshold, two gradient thresholds and probe-bubble collision period.

Such a method was required because of the complexity of the collision process (i.e. drying, wetting, glancing) and of the bubbly structures (e.g. bubble packet, shared interfacial film).

Experimental flow conditions

For each experiment, the receiving pool free-surface was located 0.09-m below the nozzle. The inflow conditions were partially-developed and turbulence levels of the free-stream were high (table 1). Air concentration measurements indicated a substantial aeration of the impinging jet free-surface (CHANSON and BRATTBERG 1997). Visually the jet appeared rough turbulent.

INVESTIGATIONS OF THE VERY-NEAR FLOW FIELD

Definition

The very-near flow field is defined as the region in which the flow characteristics are dominated by air entrapment and the interactions between gas and liquid entrainment (fig. 1 and 2). Several researchers mentioned such a flow region (Table 2).

Dominant features of the very-near-flow field include the induction trumpet and the air cavity at jet impingement (thickness δ_{al}, length x_{al}) (fig. 2). Experimental observation are summarised in Table 3. Note the scatter of the experimental data and the discrepancy between theoretical and experimental results.

In the present study, the very-near flow field corresponds to $(x-x_1)/d_1 < 5$.

Mean flow properties

Distributions of air content, mean air-water velocity and bubble frequency were recorded with the conductivity probes. Although the data exhibit some scatter, the profiles are reasonably smooth despite the proximity of the singular impingement point (fig. 3). These results were observed consistently for $(x-x_1) \geq 0.005$ m and $V_1 > 2$ m/s (CHANSON and BRATTBERG 1997).

At low inflow velocities ($V_1 \leq 2$ m/s) and for $(x-x_1) <$ 0.05 m, the flow field is highly perturbed by the individual entrainment of air bubbles, and the data exhibit a broad scatter (i.e. noise) without smooth trend.

The distributions of air bubble frequency have a maximum in the mixing layer. This maximum value tends to increase with the distance from the impingement point in the very-near flow field, indicating an increase in the number of bubbles as the largest entrained bubbles are broken up in the shear layer.

Table 1- Experimental flow conditions (supported jet, θ = 89 degrees, W = 0.269 m)

Ref.	Run	q_w	V_1	x_1 ([a])	d_1	Comments
		m^2/s	m/s	m	m	
(1)	(2)	(3)	(4)	(5)	(6)	(6)
CHANSON (1995)	F1	0.024	2.36	0.090	0.0102	Tu=1.70 %.
	F2	0.048	4.06	0.090	0.0118	Tu=1.50 %.
	F3	0.072	5.89	0.090	0.0122	Tu=0.74 %.
	F4	0.096	8.0	0.090	0.012	
	F5	0.108	9.0	0.090	0.012	
CUMMINGS (1996)	2-m/s	0.024	2.39	0.0875	0.010	Tu=1.6 %.
	6-m/s	0.072	6.14	0.0875	0.0117	Tu=0.75 %.
CHANSON and BRATTBERG (1997)	TBPJ2	0.017	2.0	0.09	0.0090	Tu=1.7 %.
	TBPJ3	0.032	3.0	0.09	0.0110	Tu=2.6 %.
	TBPJ4	0.045	4.0	0.09	0.0116	Tu=2.8 %.
	TBPJ5	0.058	5.0	0.09	0.0119	Tu=2.5 %.
	TBPJ6	0.07	6.0	0.09	0.0120	
	TBPJ7	0.082	7.0	0.09	0.0121	
	TBPJ8	0.094	8.0	0.09	0.0121	
Present study	HF-2	0.017	2.0	0.09	0.0090	Tu=1.7 %.
	HF-3	0.032	3.0	0.09	0.0110	Tu=2.6 %.
	HF-4	0.045	4.0	0.09	0.0116	Tu=2.8 %.

Notes : ([a]) : distance between nozzle and pool free-surface; W : channel width; θ : jet angle with horizontal; Tu : jet turbulence intensity at impact (measured outside of jet support boundary layer).

Velocity distributions

Mean water velocities and water velocity fluctuations, recorded with the hot-film probe, are shown in figure 4.

First note the smooth shape of the mean water velocity distributions : i.e., the same shape as monophase flows. The data scatter is comparable between conductivity probes (e.g. CHANSON and BRATTBERG 1997) and hot-film probe data (Present study), suggesting that the scatter is related to the flow behaviour rather than to the instrumentation.

Secondly let us observe the very-high level of turbulence in the shear flow. Maximum turbulent intensities of more than 100% are observed for $(x-x_1)/d_1 \le 3$. In monophase mixing layers, experimental data indicated $(Tu)_{max}$ = 15 to 20% for $(x-x_1)/d_1 \le 4$ (e.g. DAVIES 1966, SUNYACH and MATHIEU 1969, WYGNANSKI and FIEDLER 1971).

The writers analysed further the velocity probability distribution function (pdf) in the mixing layer downstream of the impingement point. The results indicate that, at any position {x,y} in the mixing layer, the distribution of velocity around the mean is neither random nor skewed. It is characterised by two peaks corresponding to a major value and a minor velocity (fig. 5).

It is believed that the high levels of turbulence in the mixing layer of developing plunging jet flow are caused by the fluctuating nature of the air entrapment process. The probe, fixed in space, is sometimes in the potential core flow ($V = V_1$) while some other times in the induction trumpet flow ($V = V_i$). When the probe tip is located in an air packet, the probe signal is not meaningful and it is discarded. Hence the two characteristic velocities, seen in figure 5, are the inflow velocity V_1 and the induction trumpet velocity V_i.

DISCUSSION

Although the shape of void fraction and mean velocity distributions suggest a smooth flow transition between the high-velocity and low-velocity regions, the air-water mixing layer is highly unstable. The air entrapment/entrainment process is very dynamic and interacts substantially with the transfer of momentum across the mixing layer.

Characteristics of the near-entrapment region were recorded for $2 \le V_1 \le 4$ m/s. The results are summarised in Tables 3 and 4. The latter gives the upper and lower boundaries of the mixing layer region in which the velocity probability distribution function exhibits two peaks (fig. 5), and the deduced induction trumpet velocity.

The results indicate that the induction trumpet velocity is a function of the inflow velocity. For the experiments, it is best correlated by :

$$V_i = 0.6684 * (V_1 - V_e)^{0.1456} \quad (1)$$

where V_e is the onset velocity of air entrainment (Table 4).

The boundaries of the two-velocity peaks pdf region are best correlated by :

$$\frac{Y_1}{d_1} = 0.04375 * \frac{x-x_1}{d_1} + 0.2115*(V_1-V_e) + 0.593 \quad (2)$$

$$\frac{Y_2}{d_1} = 1.307 * (V_1 - V_e)^{0.139} \quad (3)$$

For $Y_1 \le y \le Y_2$, the velocity probability distribution function has the shape illustrated in figure 5.

Table 2- Investigations of the very-near flow field

Ref. (1)	Investigations (2)	Comments (6)
EXPERIMENTAL OBSERVATIONS		
LIN and DONELLY (1966)	Study of air cavity length	Circular vertical jets (∅ = 4 to 8 mm).
SUCIU and SMIGELSHI (1976)	Study of air cavity length	Circular water jets (∅ = 1 to 4 mm). V_1 = 2.5 to 9.6 m/s.
KENNEDY and BURLEY (1977)	Study of air cavity length	Impingement of a solid surface in liquid.
EVANS (1990)	Study of air cavity thickness and induction trumpet	Circular plunging jet columns (∅ = 2.4 to 7.1 mm).
KUSABIRAKI et al. (1990)	Study of air cavity length	Inclined circular jets (∅ = 7 to 12 mm).
CHANSON (1995)	Study of air entrapment region	Bubble break-up region. Two-dimensional supported water jets.
CUMMINGS and CHANSON (1997)	Study of air entrapment region and air cavity thickness	Very-near flow field. Two-dimensional supported water jets.
Present study	Study of air entrapment region and induction trumpet flow	Two-dimensional supported water jets.
THEORETICAL CALCULATIONS		
SENE (1988)	Analysis of air entrapment region	
LEZZI and PROSPERETTI (1991)	Analysis of air entrapment region	Air entrainment instability caused by gas viscosity.
BONETTO et al. (1994)	Analysis of air entrapment region	Gas entrainment induced by Helmholtz-Taylor instability. Assume wave celerity equal to jet velocity.

SUMMARY AND CONCLUSION

Downstream of the impingement point of a plunging jet, the developing flow is characterised is characterised by a very-near flow region in which the flow properties are strongly affected by the entrapment conditions and an air bubble diffusion region downstream.

In the very-near flow field (i.e. $(x-x_1)/d_1 < 5$), the distributions of air content and mean velocity exhibit a smooth shape, and high levels of turbulent velocity fluctuations are recorded. The instantaneous fluctuations of the velocity are not random. In the mixing layer the velocity pdf exhibits two characteristic peaks : the inflow velocity V_1 and the induction trumpet V_i.

Characteristics of the very-near flow field were recorded and compared with existing data. The scatter of the results reflects a lack of understanding of the basic air entrapment mechanisms and of the interactions between the mixing layer and the air diffusion process. The writers hope that the present study will assist future works.

ACKNOWLEDGMENTS

The writers thank Professor C.J. APELT for his support all along the project.

REFERENCES

BIN, A.K. (1993). "Gas Entrainment by Plunging Liquid Jets." *Chem. Eng. Science*, Vol. 48, No. 21, pp. 3585-3630.

BONETTO, F., DREW, D., and LAHEY, R.T. Jr (1994). "The Analysis of a Plunging Liquid Jet - The Air Entrainment Process." *Chem. Eng. Comm.*, Vol. 130, pp.11-29.

CHANSON, H. (1995). *Report CH46/95*, Dept. of Civil Engrg., Univ. of Queensland, Australia, June, 368 pages.

CHANSON, H. (1997). "Air Bubble Entrainment in Free-Surface Turbulent Shear Flows." *Academic Press*, London, UK, 401 pages.

CHANSON, H., and BRATTBERG, T. (1997), *Report CH48/97*, Dept. of Civil Engrg., Univ. of Queensland, Australia, Oct., 309 pages.

CUMMINGS, P.D. (1996). "Aeration due to Breaking Waves." *Ph.D. thesis*, Dept. of Civil Engrg., University of Queensland, Australia.

CUMMINGS, P.D., and CHANSON, H. (1997). "Air Entrainment in the Developing Flow Region of Plunging Jets. Part 1 Theoretical Development." *Jl of Fluids Eng.*, Trans. ASME, Vol. 119, No. 3, pp. 597-602 (ISSN 0098-2202).

DAVIES, P.O.A.L. (1966). "Turbulence Structure in Free Shear Layers." *AIAA Jl*, Vol. 4, No. 11, pp. 1971-1978.

EVANS, G.M. (1990). "A Study of a Plunging Jet Bubble Column." *Ph.D. thesis*, Univ. of Newcastle, Australia.

KENNEDY, B.S., and BURLEY, R. (1977). "Dynamic Fluid Interface Displacement and Prediction of Air Entrainment." *Jl Colloid and Interface Science*, Vol. 62, No. 1, pp. 48-62.

KUSABIRAKI, D., MUROTA, M., OHNO, S., YAMAGIWA, K., YASUDA, M., and OHKAWA, A. (1990). "Gas Entrainment Rate and Flow Pattern in a Plunging Liquid Jet Aeration System using Inclined Nozzles." *Jl. of Chem. Eng. of Japan*, Vol. 23, No. 6, pp. 704-710.

LEZZI, A.M., and PROSPERETTI (1991). "The Stability of an Air Film in a Liquid Flow." *Jl of Fluid Mech.*, Vol. 226, pp. 319-347.

LIN, T.J., and DONNELLY, H.G. (1966). "Gas Bubble Entrainment by Plunging Laminar Liquid Jets." *AIChE Jl*, Vol. 12, No. 3, pp. 563-571.

SENE, K.J. (1988). "Air Entrainment by Plunging Jets." *Chem. Eng. Science*, Vol. 43, No. 10, pp. 2615-2623.

SUCIU, G.D., and SMIGELSHI, O. (1976). "Siize of the Submerged Biphasic Region in Plunging Jet Systems." *Chem. Eng. Sc.*, Vol. 31, No. 12, pp. 1217-1220.

SUNYACH, M., and MATHIEU, J. (1969). "Zone de Mélange d'un Jet Plan. Fluctuations Induites dans le Cone à Potentiel-Intermittence." ('Mixing Zone of a Plane Jet. Fluctuations Induced in the Potential Core by Random Boundary Motion.') *Intl Jl of Heat and Mass Transfer*, Vol. 12, pp. 1679-1697 (in French).

WYGANSKI, I., and FIEDLER, H.E. (1970). "The Two-Dimensional Mixing Region." *Jl of Fluid Mech.*, Vol. 41, Part 2, pp. 327-361.

Table 3- Characteristics of the very-near flow field

Ref.	Very-near flow field region $(x-x_1)$ m	Air cavity thickness δ_{al} m	Air cavity length x_{al} m	Induction trumpet velocity V_i m/s	Comments
(1)	(2)	(3)	(4)	(5)	(6)
EXPERIMENTAL OBSERVATIONS					
LIN and DONELLY (1966)			0 to 4.5 mm		Circular vertical jets (∅ = 4 to 8 mm).
SUCIU and SMIGELSHI (1976)			4 to 5 mm		Circular water jets (∅ = 1 to 4 mm). V_1 = 2.5 to 9.6 m/s.
KENNEDY and BURLEY (1977)			$\propto V_1^{0.6}$		Impingement of a solid surface in liquid.
EVANS (1990)		0.07 to 0.45 mm ([a]) [V_1=4.7 to 15 m/s]		0.6 to 2.7 ([b]) [V_1=4.7 to 15 m/s]	Circular plunging jet columns (∅ = 2.4 to 7.1 mm).
KUSABIRAKI et al. (1990)			$6*\varnothing_1$ [$2<V_1<13.5$ m/s]		Inclined circular jets (∅ = 7 to 12 mm).
CHANSON (1995)	< 50-100 mm				Bubble break-up region. Two-dimensional supported water jets.
CUMMINGS and CHANSON (1997)	< 20 mm [$2 < V_1 < 6$ m/s]	0.5 to 5 mm [$3 < V_1 < 6$ m/s]			Very-near flow field. Two-dimensional supported water jets.
Present study	$(x-x_1)/d_1 \le 5$	(as above)		0.5 to 0.8 [V_1 = 2 to 4 m/s]	Two-dimensional supported water jets.
THEORETICAL CALCULATIONS					
SENE (1988)		$\propto \frac{Q_{air}}{V_1}$ $\sqrt{\frac{2*\mu_{air}*V_1}{\rho_w*g}}$			High velocity two-dimensional jets.
LEZZI and PROSPERETTI (1991)	10 mm	< 52 μm [air & water]		0	Air entrainment instability caused by gas viscosity.
BONETTO et al. (1994)		$\propto \frac{Q_{air}}{V_1}$		V_1	Gas entrainment induced by Helmholtz-Taylor instability. Assume wave celerity equal to jet velocity.

Notes : ([a]) measured data; ([b]) calculated; [Impact flow conditions in brackets].

Table 4 - Experimental observations of the very-near flow field : dual-velocity peak flow region

Ref.	Run	$x - x_1$ m	Y_1 m	Y_2 m	V_i m/s	Comments
(1)	(2)	(3)	(4)	(5)	(6)	(6)
Present study	HF-2	0.02	0.0077	0.0141	0.65	
		0.03	0.0081	0.0094	0.65	
	HF-3	0.02	0.0121	0.0148	0.72	
		0.03	0.0134	0.0166	.072	
		0.05	0.0139	0.014	0.84	
	HF-4	0.02	0.0146	0.0193	0.60	
		0.03	0.0147	0.017	0.66	
		0.05	0.0156	0.0177	1.03	

Note : Y_1, Y_2 : upper and lower boundaries of the dual-velocity region; V_i : induction velocity (minor velocity) measured in the very-near flow field.

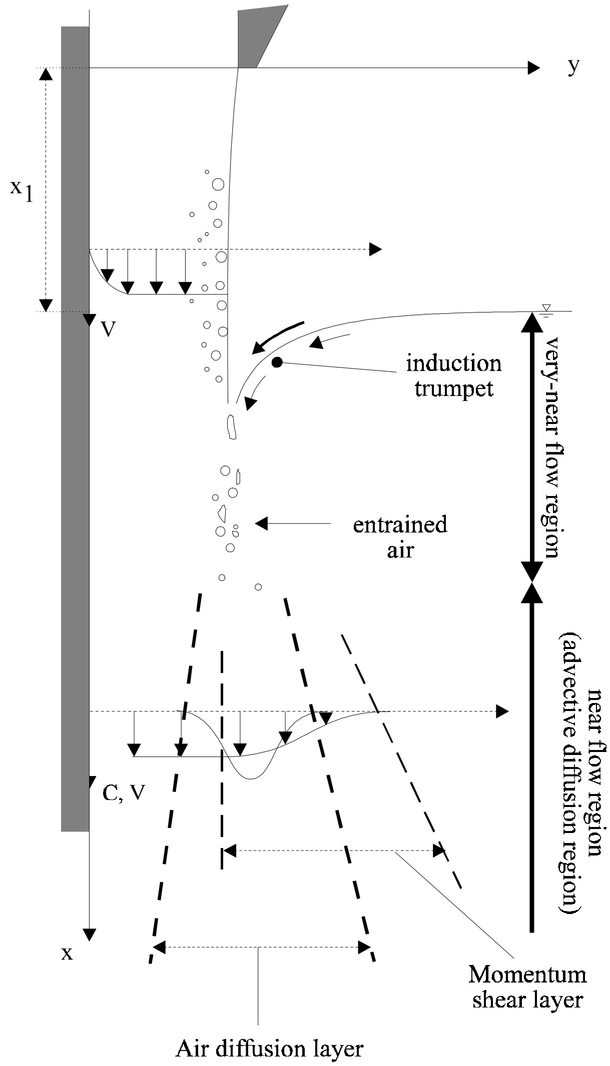

Fig. 1 - Sketch of the plunging jet apparatus at the University of Queensland

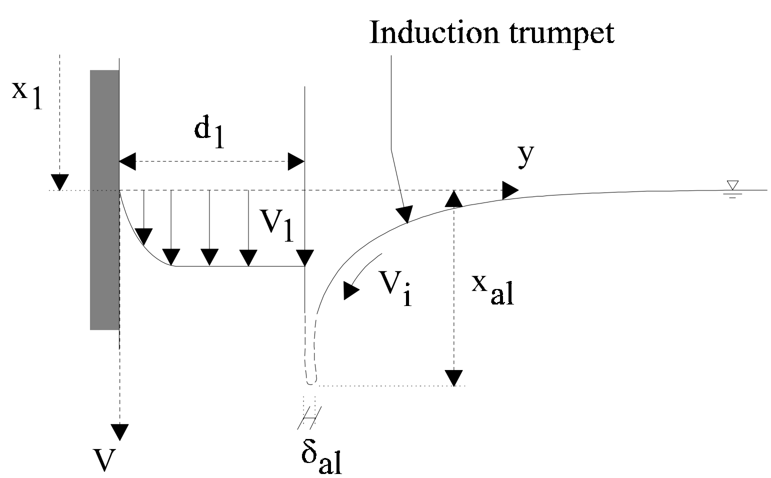

Fig. 2 - Sketch of the impingement region

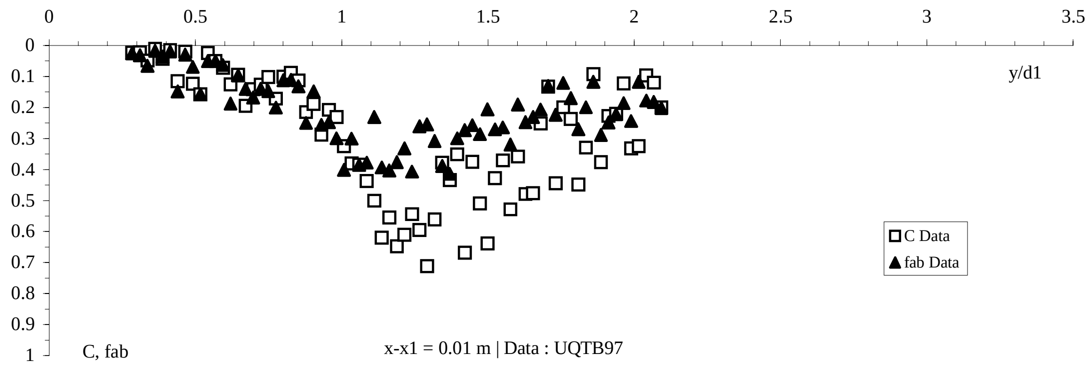

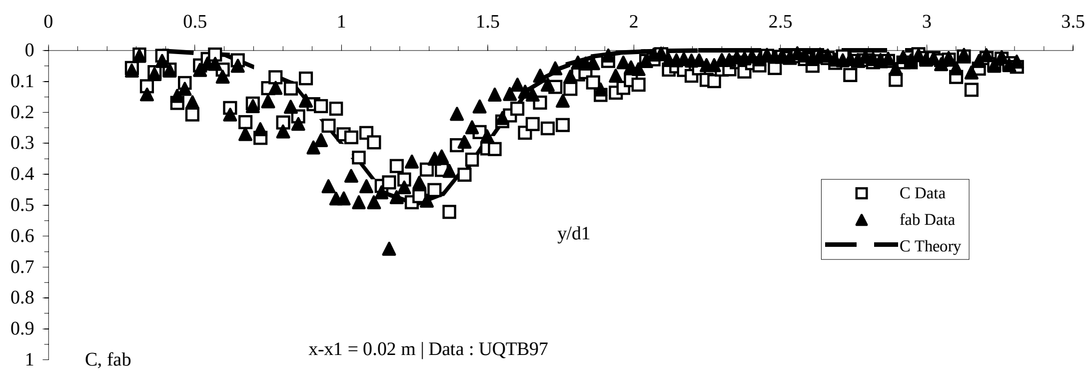

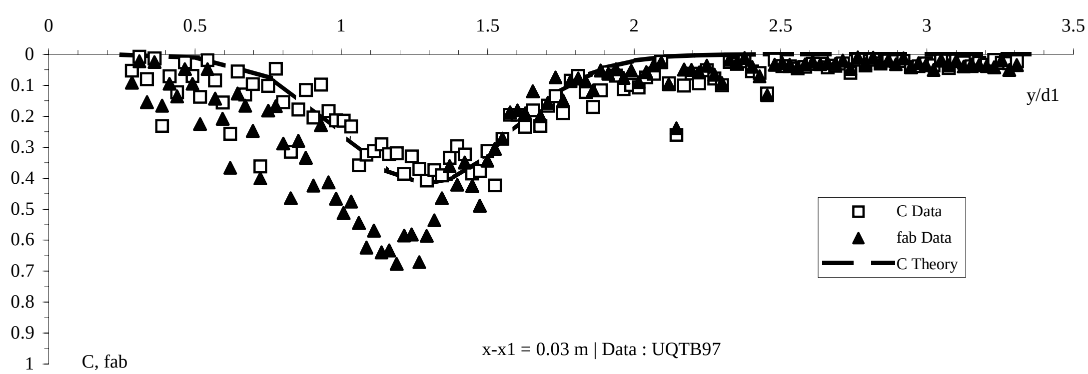

Fig. 3 - Distributions of air content and dimensionless bubble frequency (fab = F^*d_1/V_1) near the impingement point (Conductivity probe data) - Run TBPJ4, V_1 = 4 m/s, d_1 = 0.012 m, x_1 = 0.09 mm

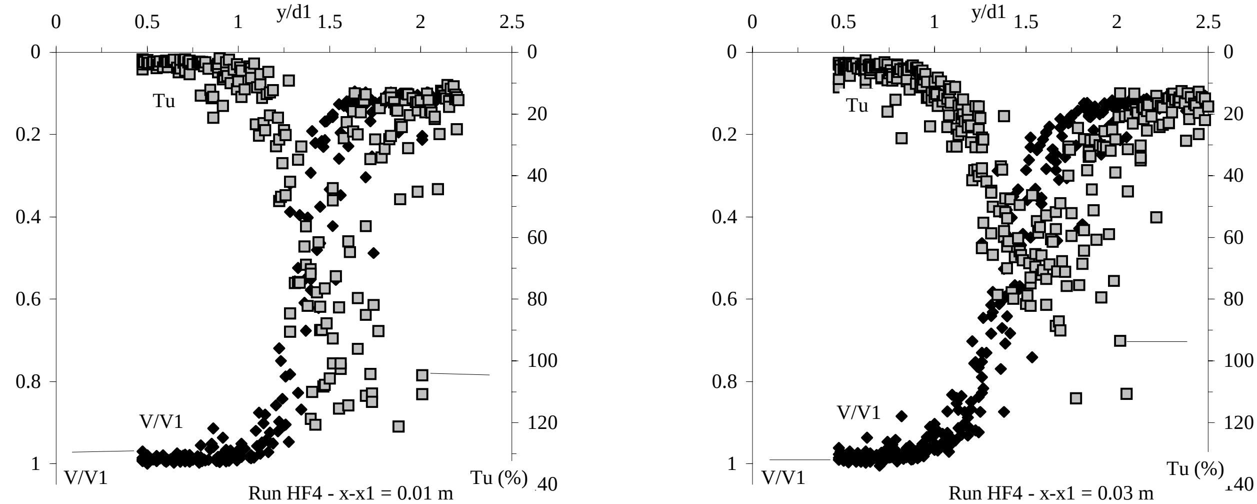

Fig. 4 - Distributions of mean water velocity and water velocity fluctuation near the impingement point (Hot-film probe data) - Run HF4, V_1 = 4 m/s, d_1 = 0.012 mm, x_1 = 0.09 mm

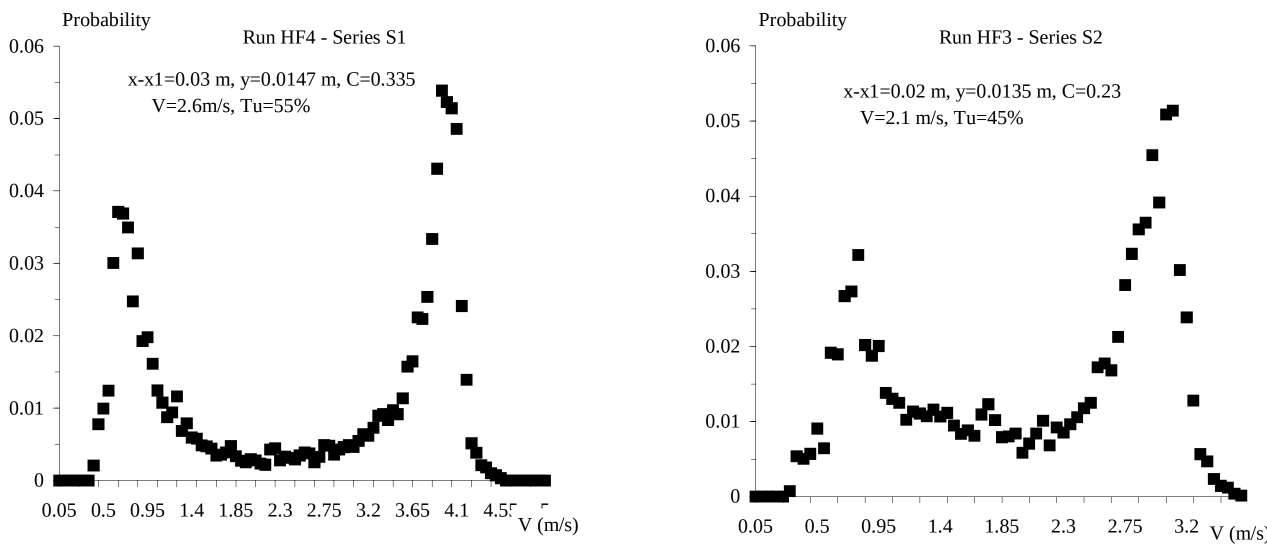

Fig. 5 - Probability distribution functions of water velocity near the impingement point (0.05-m/s intervals)